Gas properties in the Early Universe deciphered from spectral line surveys of high-z objects: The Cloverleaf Quasar

Michel Guélin[1,*], *Carsten* Kramer[1], *Chentao* Yang[2], *Belén* Tercero[3], and *José* Cernicharo[4]

[1]Institut de RadioAstronomie Millimétrique, 300 rue de la piscine, 38240 St. Martin d'Hères, France
[2]Department of Space, Earth and Environment, Chalmers University of Technology, Onsala Space Observatory, 439 92 Onsala, Sweden
[3]Observatorio Astronomico de Yebes, IGN, Cerro de la Palera, Guadalajara, Spain
[4]Instituto de Fisica Fundamental, CSIC, Serrano 121, Madrid, Spain

Abstract. Molecular lines observed in remote quasars arise from exceptionnally strong starburst regions in the vicinity of the QSO. Their study offers a unique opportunity to probe the gas physical and chemical properties at the epoch of peak star formation (z=2-3). We report the preliminary results of an on-going mm/sub-mm spectral line survey of the Cloverleaf Quasar (z=2.6), the archetype of gravitationally lensed quasars. We identify 14 molecular species, including rare isotopologues of CO and HCO^+. The high gas density tracers HCO^+, HCN, HNC and CN are detected through several rotational transitions, up to J=8-7 ($E_{up}/k \simeq 155$ K). Their emission appears to arise from dense ($> 10^6$ cm^{-3}) gas clumps embedded in a circumnuclear disk with a flat rotation curve.

1 Introduction and Observations

The Cloverleaf Quasar (H1413+117) is the archetype of gravitationally lensed quasars and one of the most luminous and best studied objects in the distant, hence young Universe. The quasar redshift (z=2.5579, as derived from a Gaussian fit to the CO J=3-2 line of figure 2) implies 11 billion years of light travel time to the Sun and an age of about 2 Gyr after the appearance of the very first stars. Located at the center of a starburst galaxy, its radiation, viewed from the Earth, is magnified by a factor as large as 11 (according to lensing models [8]) by 2 galaxies, with redshifts z≃1 and 2, respectively, that intercept the line of sight and split the quasar image into 4 distinct components (figure 1).

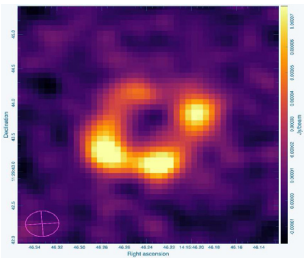

Figure 1. The Cloverleaf Quasar continuum emission at 230 GHz observed with ALMA. Image size is 2.5″, its resolution 0.3″ × 0.4″. *Acknowledgement: This paper makes use of the following ALMA data: ADS/JAO.ALMA 2011.0.01234.S and 2017.0.1232.S. ALMA is a partnership of ESO, NSF (USA), and NINS (Japan), together with NRC(Canada), MOST and ASIAA (Taiwan), KASI (Republic of Korea), in cooperation with the Republic of Chile. The Joint ALMA Observatory is operated by ESO, AUI/NRAO and NAOJ.*

The quasar and its host galaxy have been studied in the X-ray, optical and radio domains, and more particularly at sub-millimetre wavelengths. The detection of low-J lines of CO,

*e-mail: guelin@iram.fr

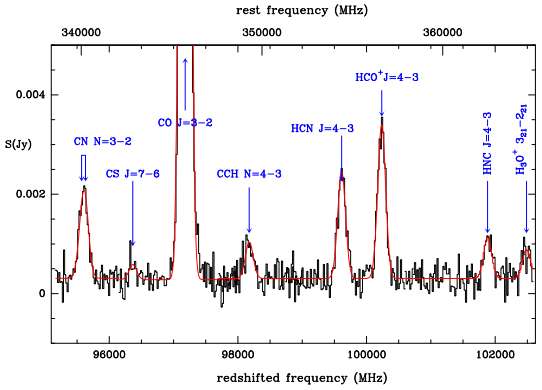

Figure 2. ALMA 3-mm spectrum of the Cloverleaf Quasar. Lower scale is redshifted frequency and upper scale rest frequency. Ordinate is line flux density in janskys. The red curve shows Gaussian fits to the detected lines. For the weakest lines, the Gaussian FWHM was set equal to that of the strongest nearby lines – see Fig. 4.

HCN and HCO^+ was reported in the early 2000s [1, 2, 5, 7], whereas a low spectral resolution survey of the 680-1100 GHz band (rest frequencies), carried out at the CSO ([3]), allowed to detect the J=6-5 through J=9-8 lines of CO. We report here the results of an on-going spectral line survey of this quasar in the mm-sub/mm domain (from 100 to 800 GHz, rest frequencies) aimed at studying the physical conditions and chemical composition of the gas in the quasar surroundings.

The survey is carried on with NOEMA, ALMA and the IRAM 30-m and Yebes 40-m telescopes. It benefits from a high spectral resolution (few MHz) and a high sensitivity (10 times higher than the pioneering work of Barvainis et al. [2]). So far, it covers the 110-180 GHz (rest frequencies) band, observed with the 40-m telescope, the 340-370 GHz band, observed with the 30-m telescope, NOEMA and ALMA, as well as the 525-625 GHz band and most of the 700-785 GHz band, observed with NOEMA.

Figures 2 and 3 show some of the ALMA and NOEMA spectra. A degree 1 baseline has been subtracted from each spectrum to remove the continuum. The r.m.s. noise per 80 kms^{-1} channel is 0.3-0.5 mJy. The NOEMA on-source integration time was 8 hours per pair of 8 GHz-wide spectra.

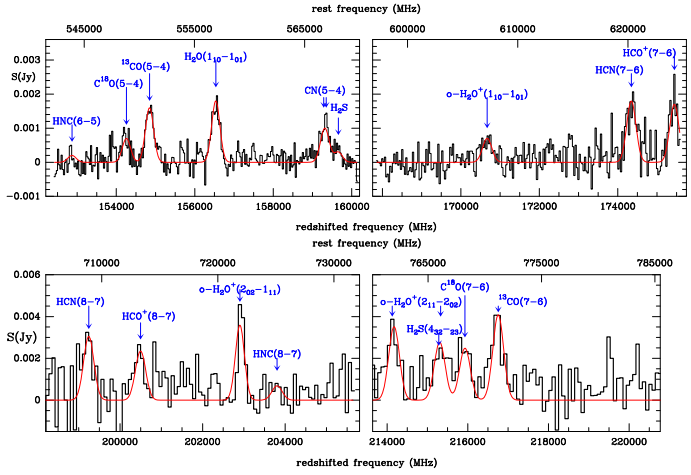

Figure 3. NOEMA 2-mm and 1-mm spectra of the Cloverleaf Quasar. As in Fig. 2, the red curves show Gaussian fits to the detected lines, the Gaussian FWHM of the weakest lines being set equal to that of the strongest nearby lines. Note the detections of H_2O, H_2O^+, H_2S and of the rare isotopologues $C^{18}O$ and ^{13}CO.

2 Results

Fourteen molecular species, including the rare CO isotopologues ^{13}CO and $C^{18}O$ and the rare HCO^+ isotopologue $H^{13}CO^+$, are detected. Three species, CH, CCH, and H_2O^+, are

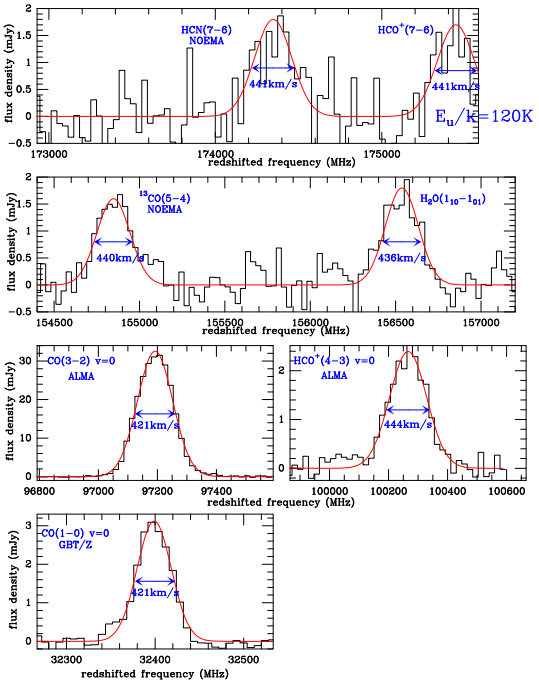

Figure 4. Line profiles of the strongest lines detected in the Cloverleaf Quasar. Red curves show the fits by a Gaussian whose FWHM is marked in blue. The upper 6 profiles are extracted from the spectra of Figs. 2 and 3, and the CO(1-0) line profile from GBT observations ([6]).

.

characteristic of gas irradiated by stellar UV, i.e. of diffuse clouds. The others species, CO, CS, HCN, HNC, HCO^+ H_2O, H_3O^+ and H_2S, are more typical of UV-shielded clouds.

The low noise level and the flat baselines provided by the interferometers allow an accurate determination of the shapes and strengths of the strongest lines (figure 4). The CO(3-2) line, which has the highest S/N, exhibits an almost perfect gaussian shape with a full width at half power of 421 ± 50 kms^{-1}. This is the same width as the CO(1-0) line and, within the errors, as the much weaker, but optically thin, ^{13}CO(5-4) line (440 ± 100 kms^{-1}) — note that the CO(7-6) line reported by [1] was observed with an insufficient bandwidth and that the higher-J CO lines were observed with a too coarse spectral resolution [3].

The lines of the high gas density tracers HCN, HCO^+ and H_2O seem to be marginally wider (FWHP $\simeq$ 440 ± 100 kms^{-1}), but still compatible with the CO linewidths. The line intensities are far better determined than in previous measurements. The CO(3-2) line luminosity (hence the observed source brightness temperature) is found to be definitely stronger (by 15%) than that of the (1-0) line. This and the near equality of the ^{13}CO(5-4) and (7-6) line brightness temperatures imply a warmer and/or denser gas than previously assumed (30-50 K, 10^{3-5} cm^{-3} according to [6, 9]) and refute the hypothesis that CO lines arise from an homogeneous gaseous disk. As for the dust grains, the SED of the mm/sub-mm continuum [9] is best fitted by a 3-component model with a cold component at 30 K, a lukewarm component at 50 K and a hot component at 115 K, the latter representing only $\simeq$ 1% of the total dust mass. The detections of several transitions of the high density tracers HCO^+, HCN, HNC and CN, as well as that of the rare isotopologues ^{13}CO and $H^{13}CO^+$ (whose lines have opacities <1) allow us to disentangle the relative contributions of the gas kinetic temperature, H_2 volume density, infrared pumping and line opacity to the line strengths, hence to better constrain the molecular gas properties.

Figure 5 shows the HCO^+, HCN and HNC velocity-integrated line flux density divided by J^2_{upper} (i.e. a quantity that scales with the line luminosity L'), as a function of J_{upper}.

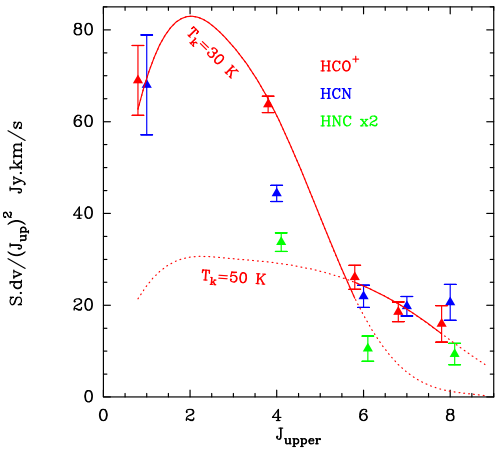

Figure 5. The velocity-integrated flux density of the lines of the high density tracers HCO^+, HCN and HNC, divided by J^2_{upper}. Abscissa is J_{upper}. The two red curves show fits to the low-J and high-J HCO^+ lines, respectively, with an LVG statistical equilibrium code (MADEX [4]). The fits require 2 different gas temperatures.

Two main results stem from this figure. The first is that fluorescent excitation, via infrared pumping, does not play a major role througout the molecular disk, contrary to what is argued for some superluminous infrared galaxies (e.g. APM08279+5255). The HNC molecule, which has the lowest vibrationally excited state ($v2(1-0) = 21.7\mu$m above the ground state, a wavelength close to the peak of the dust continuum SED), should be the most affected by such a pumping. In contrast, the lowest bending states of HCN ($v2(1-0) = 14.0\mu$m), and HCO^+ ($v2(1-0) = 12.1\mu$m), are shifted to wavelengths at which the continuum flux is reduced by factors 6-8. Yet, HCN is the molecules whose luminosity decreases the slowest. In the same vein, despite the lack of bending states for CN, the HCN/CN luminosity ratio remains constant from 350 GHz to 600 GHz, when IR pumping should have strongly increased it.

The second result is that the HCN line luminosity remains almost constant between the J=6-5 and the J=8-7 lines, despite the fact that the latter levels lie twice higher in energy than the former ones. Similarly, the ^{13}CO(5-4) line luminosity is not significatively lower than that of ^{13}CO(7-6). This contrasts with the factor of 2 decrease in luminosity between HCN(4-3) and HCN(6-5), and the factor of 1.7 decrease between CO(3-2) and CO(5-4). A probable explanation is that the gas kinetic temperature and the dust temperature increase from the edges of the extended starburst region (whose radius is 700 pc according to [8]) to the quasar immediate surroundings. This is illustrated by the fits to the HCO^+ lines in Fig. 5 with an LVG model, which require at least two different temperatures. That the linewidths do not significantly change from line to line suggests that the starburst region is a clumpy gaseous disk rotating around the central quasar with a nearly flat rotation curve.

References

[1] Alloin, D., Guilloteau, S., Barvainis, R. et al., A&A **321**, 24-28 (1997)
[2] Barvainis, R., Maloney, P., Antonucci, R., Alloin, D., ApJ **484**.695-701 (1997)
[3] Bradford, C.M., Aguirre, J.E., Aikin, R. et al., ApJ **2009**, 112=122 (2009)
[4] Cernicharo, J., Laboratory astrophysics and astrochemistry in the Herschel/ALMA era, ECLA, EAS Pub. Series **58**, 251-261 (2012)
[5] Riechers, D.A., Walter, F., Carilli, C.L. et al., ApJL **645**, L13-L16 (2006)
[6] Riechers, D.A., Carilli, C.L., Maddalena, R.J. et al., A&A **ApJ**, L32-39 (2011)
[7] Solomon, P., Vanden Bout, P., Carilli, C. and Guélin, M., Nature **426**, 636 (2003)
[8] Venturini, S. and Solomon, P.M., ApJ **540**, 740-745 (2003)
[9] Weiss, A. et al., A&A **409**, L41-L45 (2003)